High efficiency event-counting thermal neutron imaging using a Gd-doped micro-channel plate*

TIAN Yang(田阳)[1,2;1)] YANG Yi-Gang(杨祎罡)[1,2] PAN Jing-Sheng(潘京生)[3]
LI Yu-Lan(李玉兰)[1,2] LI Yuan-Jing(李元景)[1,2]

[1] Department of Engineering Physics, Tsinghua University, Beijing 100084, China
[2] Key Laboratory of Particle & Radiation Imaging (Tsinghua University), Ministry of Education, Beijing 100084, China
[3] Nanjing Branch, North Night Vision Tech. Co., Ltd., Nanjing 211102, China

Abstract: An event-counting thermal neutron imaging detector based on 3 mol % $^{nat}Gd_2O_3$-doped micro-channel plate (MCP) has been developed and tested. A thermal neutron imaging experiment was carried out with a low flux neutron beam. Detection efficiency of 33% was achieved with only one doped MCP. The spatial resolution of 72 μm RMS is currently limited by the readout anode. A detector with larger area and improved readout method is now being developed.

Key words: doped MCP, thermal neutron imaging, event-counting

PACS: 28.20.Pr, 29.40.Gx **DOI:** 10.1088/1674-1137/38/8/086003

1 Introduction

The concept of direct conversion and detection of thermal neutrons using doped micro-channel plates (MCPs) was first proposed by Fraser and Pearson in 1990 [1]. The first experimental imaging result was achieved using boron- and gadolinium-doped MCP by researchers from the University of California at Berkeley and Nova Scientific Inc. in 2007 [2]. High spatial and temporal resolution as well as relatively high detection efficiency was then confirmed by a series of experiments [3–5]. As a result, event-counting detectors based on doped MCPs combined with pixel readout chips have been successfully applied in various neutron imaging experiments [6, 7].

Similar research is being carried out in China by Tsinghua University and NNVT Co., Ltd. Both doping and coating have been attempted to increase the neutron sensitivity of MCPs [8]. Our coated MCPs still have the problem of integrating the electron emitting layer. The first thermal neutron imaging result of our doped MCP is presented in this paper.

2 Neutron imaging detector using a wedge strip anode

Although boron has several advantages over gadolinium in neutron conversion, such as shorter range of the charged particles (so higher spatial resolution is achievable), large cross section over the whole thermal region, and a simple prompt gamma spectrum (which makes coincidence measurements easier), highly enriched ^{10}B ($50000/kg) is needed to realize desirable detection efficiency with a practical thickness (around 1 mm) of the MCP. Doping with ^{nat}Gd is a more cost-effective choice. In our first attempt, 3 mol % $^{nat}Gd_2O_3$-doped MCP was made,with a diameter of 50 mm and thickness of 0.6 mm. The diameter and pitch of the channels are 10 and 12.5 μm respectively, with a porosity ratio of 63%.

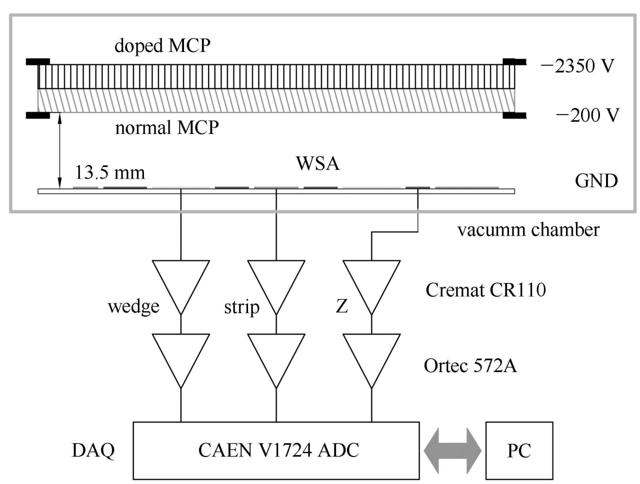

Fig. 1. The imaging detector and electronics system.

Received 21 October 2013, Revised 19 February 2014
∗ Supported by National Natural Science Foundation of China (10735020, 11075026)
1) E-mail: cycjty@126.com

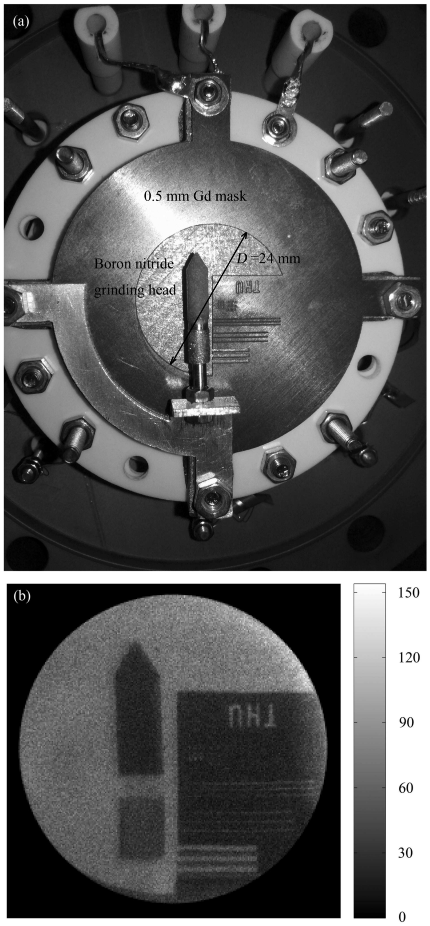

Fig. 2. Imaging objects and results. The imaging objects are fixed in the vacuum chamber. As the neutron flux is very low, in order to get imaging of desirable quality within acceptable acquisition time we selected objects of high contrast for thermal neutrons: the boron nitride grinding head and 0.5 mm Gd mask shown in (a). In (b), the pixel size is 100 μm.

Detailed composition and production procedures are given in Ref. [9].

The $^{\rm nat}$Gd-doped MCP (0° bias angle) is coupled to a normal 0.6 mm MCP (8° bias angle) in the form of a chevron stack. A wedge strip anode (WSA) [10] is employed as a 2-D event-counting readout. These are the essential parts of our neutron imaging detector as illustrated in Fig. 1. The simple electronics system of the WSA is comprised of only 3 channels.

3 Imaging with a low flux neutron beam

Thermal neutron imaging was carried out at the 49-2 reactor at the China Institute of Atomic Energy (CIAE). As the reactor is intended for isotope production and sample irradiation, there is no gamma filter in the neutron beam. The n/γ ratio is still as low as 1.07×10^{10} n/(cm^2·Sv) after 10 cm thick lead brick. This value is an order of magnitude lower than that of some neutron sources optimized for imaging [11, 12]. The thermal neutron flux within the imaging plane is just 123 n/(cm^2·s) at a L/D of 360:1 according to measurements with a ^{3}He tube.

Fortunately the dark count rate of our detector is just 0.11 s^{-1}·cm^{-2}. We managed to obtain transmission imaging of some high contrast objects (Fig. 2) after irradiating the detector for 2 hours and 39 minutes.

4 Discussion and conclusion

From Fig. 2, after removing the part due to the boron nitride grinding head, one can get a spectrum of the event density, as shown in Fig. 3. There are two well-separated peaks corresponding to two different regions: the 0.5 mm Gd blocked part and the unblocked part. Although the 0.5 mm Gd cannot effectively absorb epithermal neutrons, the absorption by the Gd doped MCP is also negligible. Thus in the blocked part it can be considered that only gamma signals and dark counts contribute to the event density. The difference between the two peaks is the net number of thermal neutron events per pixel in the open area. After comparing this value with the thermal neutron flux (123 n/(cm^2·s) with RMS deviation of 8 n/(cm^2·s)), we estimate the detection efficiency to be 33% with RMS deviation of 2%. The spatial resolution was derived by fitting the edge of the Gd mask (Fig. 4). A resolution of 72 μm RMS was achieved in the central area.

The efficiency is higher than the result measured by NOVA for Gd doped MCP [13]. Although the value of 33% is still much lower than the model-predicted 50%

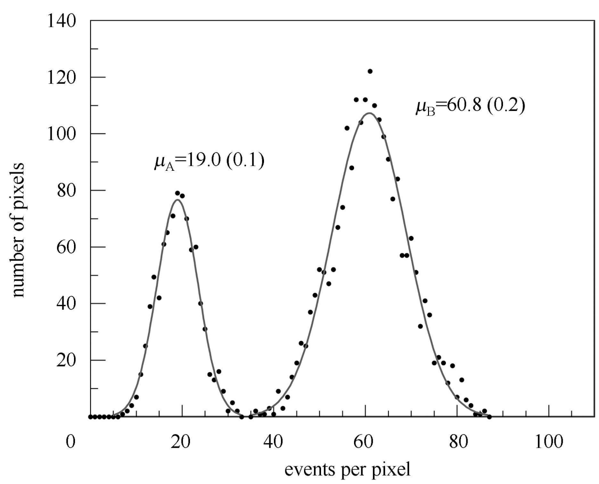

Fig. 3. The modified greyscale spectrum. This spectrum shows the event density distribution after removing the grinding head. $\mu_{\rm A}$ and $\mu_{\rm B}$ are the fitted average events per pixel in the blocked and unblocked parts respectively. The values in the brackets are the RMS deviations.

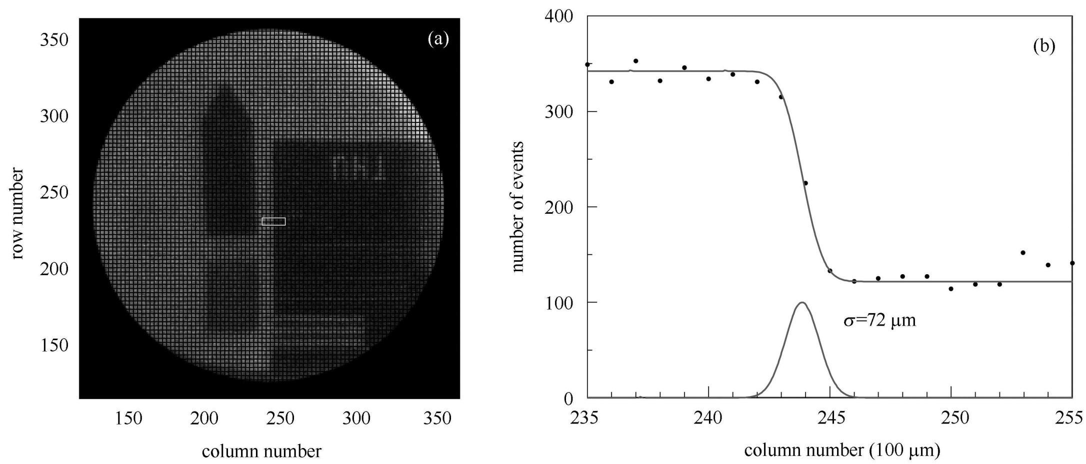

Fig. 4. The derived spatial resolution. In (a), the length of each grid is 3 pixels. The edge within the white box was fitted using error function. The number of events in (b) is the sum of 6 adjacent rows within one column. This was done to suppress the statistical fluctuation at the expense of spatial resolution loss. The RMS of the derivative (Gaussian function) is 72 μm.

for ^{10}B doped MCPs [14] (the maximum doping ratio (3%) of Gd_2O_3 for current MCP manufacturing technique is much lower than that of B_2O_3), the efficiency can be further enhanced by increasing the thickness or using a smaller channel diameter or both. According to our theoretical model, the efficiency for 25.3 meV neutrons can be increased to 62% (5 μm channel diameter and 1 mm thickness) [15].

The spatial resolution is mainly limited by the WSA. In our previous tests, the spatial resolution for 10 kVp X-rays remained at the same level. The intrinsic event centroiding uncertainty is due to the electron transport process in the MCP. According to the Monte Carlo simulation of such a process, the uncertainty is 13 μm RMS for 71.9 keV electrons. Large area Gd doped MCP (10 cm diameter) is now being developed. A 2-D delay line system will be used as its readout. Both the spatial resolution and the imaging area can be greatly improved.

The imaging result also testifies that an event-counting detector based on doped MCP is able to work with a low flux and high gamma content neutron beam. This is useful for in situ thermal neutron imaging where only mobile sources of relatively low performance are available.

In conclusion, the first event-counting imaging test of our Gd-doped MCP detector was successful. Detection efficiency as high as 33% for thermal neutrons was achieved using only a single 0.6 mm thick doped MCP. The spatial resolution of 72 μm RMS is limited by the WSA and can be greatly enhanced in future.

References

1 Fraser G W, Pearson J F. Nucl. Instrum. Methods A, 1990, **293**: 569–574

2 Siegmund O H, Vallerga J V, Tremsin A S et al. Nucl. Instrum. Methods A, 2007, **576**: 178–182

3 Tremsin A S, Vallerga J V, Mcphate J B et al. Nucl. Instrum. Methods A, 2008, **592**: 374–384

4 Tremsin A S, Mcphate J B, Vallerga J V et al. Nucl. Instrum. Methods A, 2009, **604**: 140–143

5 Tremsin A S, Mcphate J B, Vallerga J V et al. Nucl. Instrum. Methods A, 2009, **605**: 103–106

6 Siegmund O H, Vallerga J V, Tremsin A S et al. IEEE Trans. Nucl. Sci., 2009, **56**: 1203–1209

7 Tremsin A S. Neutron News, 2012, **23**: 35–38

8 TIAN Yang, LU Nian-Hua, YANG Yi-Gang et al. Realization of Neutron Sensitive MCP with ALD Technique. In: Townsend D W. Proc. of 2011 IEEE Nuclear Science Symposium. New York: Curran Associates, 2011. NP1. M-11 196–198

9 PAN Jing-Sheng, YANG Yi-Gang, TIAN Yang et al. J. Instrum., 2013, **8**: P01015

10 Martin C, Jelinsky P, Lampton M et al. Rev. Sci. Instrum., 1981, **52**: 1067–1074

11 Chiro P, Bach P, Lehmann E. Neutron Radiography Activity in the European Program Cost 524: Neutron Imaging Techniques. In: Duggan J L & Morgan I L. Proc. of the 16th Conference on Application of Accelerators in Research and Industry. Melville: AIP, 2001. CP576 1103

12 Balasko M, Kuba A, Tanacs A. Comparison Radiography and Tomography Possibilities of FRM-II (20 MW) and Budapest (10 MW) Research Reactor. In: Arif M, Downing R G. Proc. of the 8th World Conference on Neutron Radiography. Lancaster: DEStech Publications, 2006. Facilities and Instrumentation

13 Siegmund O H, Vallerga J V, Martin A et al. Nucl. Instrum. Methods A, 2007, **579**: 188–191

14 Tremsin A S, Feller W B, Downing R G. Nucl. Instrum. Methods A, 2005, **539:** 278–311

15 TIAN Yang. Event Counting Thermal Neutron Imaging Based on Neutron Sensitive Micro Channel Plate (Ph. D. Thesis). Beijing: Tsinghua University, 2012 (in Chinese)